RSC Advances

PAPER

View Article Online
View Journal | View Issue

Cite this: *RSC Adv.*, 2022, **12**, 24390

Ultrabright carbon dots as a fluorescent nano sensor for Pb^{2+} detection

Xiang Long,[a] Ruixue Li,[a] Jiamei Xiang,[a] Shaogui Wu *[a] and Jiayang Wang[b]

Received 10th June 2022
Accepted 8th July 2022

DOI: 10.1039/d2ra03591j

rsc.li/rsc-advances

In this work, we synthesized ultrabright carbon dots (U-CDs) with photoluminescence quantum yield (PLQY) up to ~100% using CA and EDA as precursors. When studying their interaction with the Pb^{2+} ion, we found that the PL quenching degree is independent of the U-CDs concentration. This feature provides great convenience for practical detection, which allows the standard curve determination and practical detection to be conducted under different U-CDs concentrations with detection error less than 20%. Based on the experimental observations, a possible mechanism is proposed to explain this phenomenon. To our best knowledge, this work has never been reported before and provides a new idea for the design of novel fluorescent sensors.

1 Introduction

The existence of some trace metal ions can greatly cause photoluminescence (PL) quenching of carbon dots (CDs). This phenomenon can be used for quantitative detection of metal ions. The relationship between fluorescence intensity I of CDs and metal ion concentration can be described by the Stern–Volmer equation:[1]

$$I_0/I = 1 + K_{SV}[Q] \quad (1)$$

where, K_{SV} is the equilibrium constant of the quenching reaction, $[Q]$ is the concentration of metal ions (quencher) and I_0 and I are the fluorescence intensity of CDs before and after reaction with metal ions, respectively. From the form of the Stern–Volmer equation, one can see that I_0/I is a ratio, theoretically independent of the value of I_0, that is, independent of the concentration of fluorescent agent. However, in most practical detections, the concentration of CDs is very important, which determines both the detection sensitivity and detection range. Generally, a higher concentration of CDs results in a wider detection range of metal ions and a lower detection sensitivity. Conversely, the smaller the concentration of CDs, the narrower the detection range of metal ions, and the higher the detection sensitivity. Therefore, it is necessary to optimize the concentration of CDs before detection. An appropriate concentration of CDs should be selected according to the need of ion concentration detection.

CDs, a new member of the family of carbon materials,[2,3] are a novel 'zero-dimensional' carbon nano fluorescent material.[4,5] Compared with traditional semiconductor quantum dots (QDs) and organic dyes, CDs offer many advantages such as good water solubility, low toxicity, and low preparation cost.[6–9] Therefore, CDs show a wide application potential in display equipment,[10–12] energy conversion,[13–15] bioimaging,[16–19] analytical detection[20–23] and other fields. Citric acid (CA) and ethylenediamine (EDA) are a famous combination of precursors that can synthesize ultrabright CDs (U-CDs) with considerable photoluminescence quantum yield (PLQY).[24,25] In this work, using CA and EDA as precursors, we synthesized U-CDs by traditional hydrothermal method with PLQY up to ~100%. When we investigated their interactions with metal ions, fluorescence quenching degree was found to be independent of the U-CDs concentration. This characteristic provides great convenience for the actual detection. It allows a long interval between the standard curve preparation and the actual measurement, and allows both to be conducted at different U-CDs concentrations, which have little influence on the accuracy of final detection result. To our best knowledge, this phenomenon has rarely been reported before. This work is of considerable practical importance for developing novel fluorescent sensors for metal ions detection.

2 Experiment

2.1 Instruments and reagents

Hydrothermal reactor (25 mL) was purchased from Anniu Technology Co., Ltd. Electric drying oven was purchased in Shanghai Lichen Technology Co., Ltd. UV-vis spectra were measured by a Shunyuhengping 756 PC UV-vis spectrophotometer, and fluorescence spectra were determined by a Shanghai Lengguang F98 fluorescence spectrophotometer.

Quinine sulfate was purchased from Shanghai Aladdin Biochemical Technology Co., Ltd. Chemical reagents such as

[a]College of Chemistry and Materials Science, Sichuan Normal University, Chengdu 610066, China. E-mail: shaoguiwu@sicnu.edu.cn
[b]Department of Resources & Environment, Chengdu University of Information Technology, Chengdu 610041, China

citric acid (CA) and ethylenediamine (EDA) were purchased from Tianjin Comiou Chemical Reagent Co., Ltd. The experimental water was self-made secondary distilled water. All ionic reagents were purchased from the National Center for Analysis and Testing of Nonferrous Metals and Electronic Materials.

2.2 Synthesis of fluorescent CDs

The U-CDs were synthesized by conventional hydrothermal method using CA and EDA as precursors. About 1 mmol CA and 9 mmol EDA was dissolved in 10 mL secondary distilled water and ultrasonicated for about 10 minutes. The mixture was then transferred to a 25 mL Teflon-lined stainless-steel autoclave and kept at 170 °C for 5 h. After that, the reactor was cooled naturally in the oven. The obtained product solution was subjected to centrifugation at 10 000 rpm for 10 min to remove insoluble solid particles. The supernatant was filtered with a 0.22 μm microporous filter to obtain a clear U-CDs solution, which was stored as stock solution in a 4 °C refrigerator for standby. The details about relative PLQY determination can be found in the literature.[26]

2.3 Structural characterization

Fourier transform infrared spectroscopy (FT-IR): U-CDs solution was placed in a vacuum oven and fully dried at 60 °C and mixed with KBr in the ratio of 1 : 100, grinded, pressed, and then FT-IR measurement was carried out with scanning range 4000–400 cm^{-1}. X-ray photoelectron spectroscopy (XPS): the surface composition of dried U-CDs was determined by a Thermo Scientific ESCALAB 250Xi X-ray photoelectron spectrometer with C 1s (284.6 eV) as the internal standard. Transmission electron microscopy (TEM): the U-CDs solution was dropped on a copper wire. After drying under light, the morphology of U-CDs was observed by a Hitachi H-7650 electron microscope.

2.4 Detection of metal ions

A cuvette was loaded with a mixture of 1 mL diluted U-CDs solution and 1 mL metal ion solution, which was kept in dark for 30 minutes and then subjected to acquisitions of UV-vis and fluorescence spectra. In metal ion selectivity experiment, the concentrations of all metal ions are 0.020 mM. In the Pb^{2+} detection experiment, the concentration of Pb^{2+} is varied from 0.002 mM to 0.364 mM. UV-vis spectra were acquired at the range of 200–800 nm with an interval of 1 nm. Fluorescence spectra were acquired at the range of 375–640 nm with the excitation wavelength of 358 nm. The scanning speed is 3000 nm min^{-1}.

3 Results and discussion

3.1 Structural characterization

Fig. 1A displays a TEM photograph of the U-CDs, which are not regular spherical, and their particle size distribution ranges from nano to micron. These features are not in line with the conventional morphology and size of U-CDs (<10 nm). In addition, there are not many particles observed under the TEM, so these particles might be not the only substance with luminous activity. Fig. 1B shows one of these particles in high-resolution. No ordered lattice could be observed, suggesting that the core of U-CDs does not have graphene structure. It is speculated that these particles might be disordered flocs formed by CA and EDA.

The functional groups of U-CDs were characterized by Fourier Transform Infrared Spectroscopy (FT-IR), as shown in Fig. 1C. The peak at 3700–3200 cm^{-1} is O–H stretching vibration peak; the peak at 3500–3300 cm^{-1} is N–H stretching vibration peak; the peak at 2923–2853 cm^{-1} is C–H stretching vibration peak; the peak at 1656 cm^{-1} is C=O (amide I) stretching vibration peak; the peak at 1564 cm^{-1} is the bending vibration peak of the N–H (amide II) on the amide bond; the peak at 1485 cm^{-1} is C–N (amide III) stretching vibration peak. The three peaks are characteristic absorption peaks of amide bond. In addition, the U-CDs may also contain $–NH_2$, –OH, and –COOH functional groups. The chemical composition and elemental composition of U-CDs were analyzed by X-ray photoelectron spectroscopy (XPS). Fig. 1D displays a wide-scan XPS spectrum of U-CDs, which shows three characteristic binding energy peaks, namely, C 1s (284.18 eV), N 1s (399.11 eV) and O 1s (530.22 eV), indicating that the U-CDs mainly contain three elements C, N and O, and the relative content ratio of C/N/O is 63.87% : 17.00% : 19.13%. Fig. 1E displays the XPS spectrum for C 1s, which contains three characteristic carbon peaks 283.91 eV (C–C/C=C), 285.29 eV (C–N), 287.03 eV (C=O). Fig. 1F is the N 1s spectrum, and two subpeaks of 398.65 eV (C–N–C) and 400.03 eV (N–H) can be resolved. Fig. 1G is the O 1s spectrum, only one characteristic peak is observed at 530.24 eV (C=O).[27]

3.2 Optical properties

The UV-vis absorption, excitation, and emission spectra of the U-CDs are shown in Fig. 2A. UV-vis absorption spectrum has two main absorption peaks at 240 nm and 360 nm respectively. The one at 360 nm is basically coincident with the excitation peak, which is the characteristic absorption peak of the U-CDs. It might be contributed by the n → π*electronic transition of the surface functional group –C=O of the U-CDs. The presence of –NH– or $–NH_2$ groups leads to the red shift of this peak. The excitation and emission spectra are basically symmetrical. The maximum excitation and emission wavelengths are 358 nm and 442 nm respectively. Furthermore, if quinine sulfate is employed as the standard reference (PL quantum yield = ~54%), one can estimate the PLQY of U-CDs (~100%) by measuring the change of integral PL intensity with absorbance, as shown in Fig. 2B. Since we have optimized the synthesis conditions of U-CDs through a fine optimization strategy, the product U-CDs have an ultrahigh PLQY.[24,25,28]

3.3 Independence on U-CDs concentration

In order to study the effect of U-CDs concentration on the degree of fluorescence quenching, we carried out three groups of experiments, where the U-CDs concentration increases from 0 μg mL^{-1} to 2.25 μg mL^{-1} in each group. The samples in the first group were blank U-CDs without addition of any metal

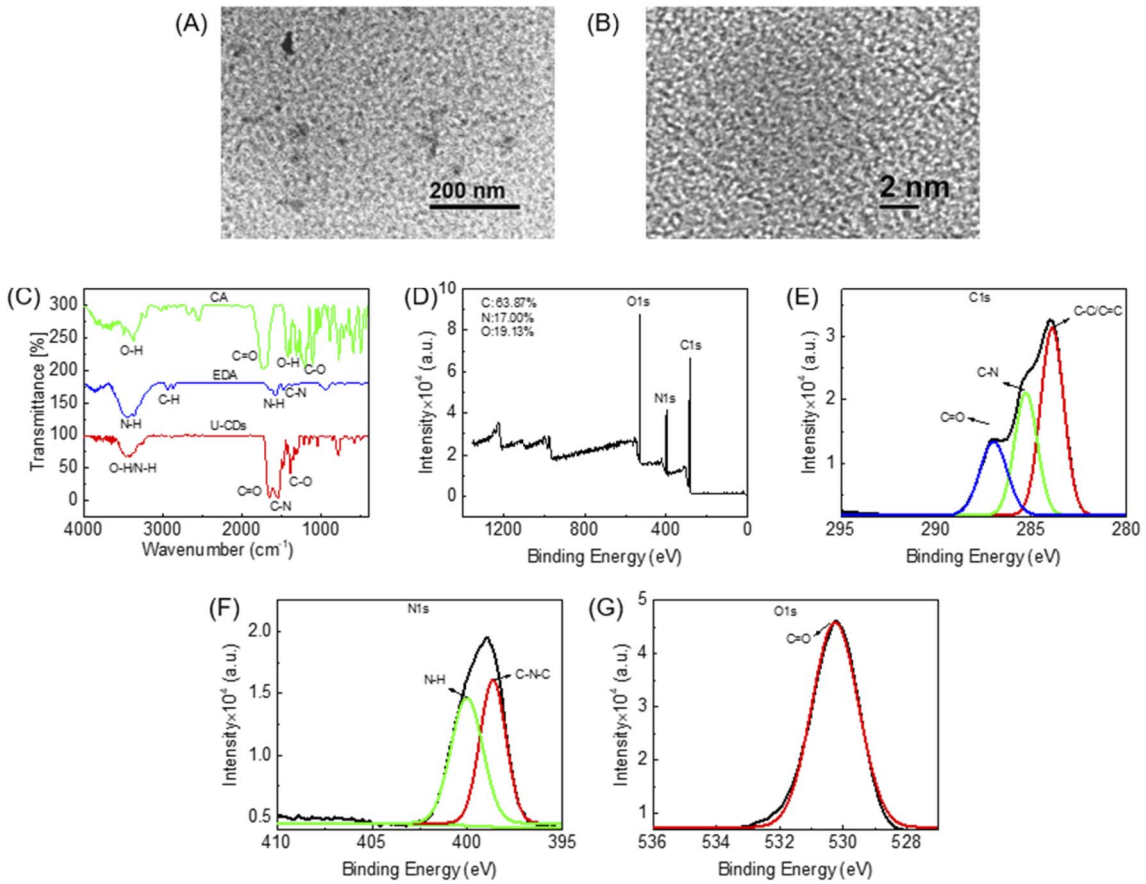

Fig. 1 Structural characterization of the U-CDs. (A) Transmission electron microscope (TEM) image. (B) A zoom-in image of a particle in 2 nm resolution. (C) FT-IR spectra of CA, EDA and the U-CDs. (D) Wide-scan XPS spectrum of U-CDs. (E–G) High resolution XPS spectra of C 1s, N 1s and O 1s, respectively.

ions. In the second group, each U-CDs sample was mixed with 0.04 mM Pb^{2+}. In the third group, each U-CDs sample was mixed with 0.4 mM Pb^{2+}. The PL spectra of three groups of U-CDs are displayed in Fig. 3A–C, respectively and their PL intensities are shown in Fig. 3D. One can clearly see that in the second group ($[Pb^{2+}] = 0.04$ mM), the PL quenching degree (PLQD) $(I_0 - I)/I_0$ remains basically unchanged with the increase of the concentration of U-CDs, as shown in Fig. 3E. When the concentration of the metal ion is increased from 0.04 mM to 0.4 mM, the PLQDs are still basically equal in the same group, as shown in Fig. 3F. This result suggests that the PLQD of U-CDs is only related to the concentration of metal ions, while almost

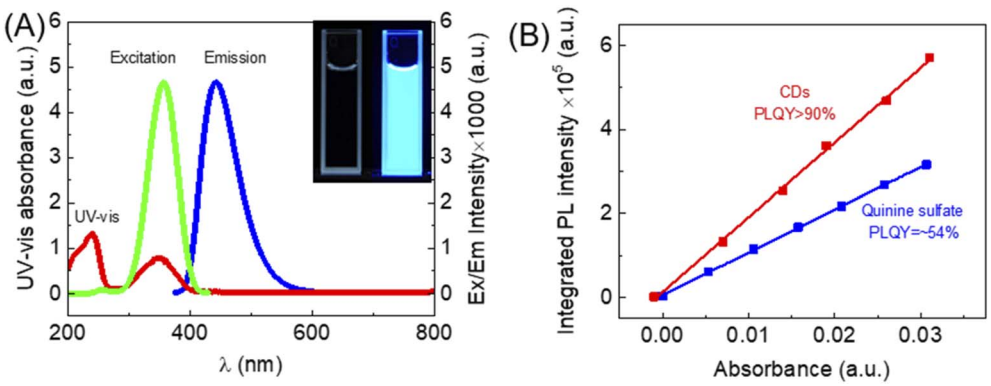

Fig. 2 Optical properties. (A) UV-vis absorption spectrum (red), excitation spectrum (green) and emission spectrum (blue) of the U-CDs. The inset displays the U-CDs under the daylight (left) and UV lamp (right), respectively. (B) Fitting curve of integrated PL intensity and UV-vis absorbance.

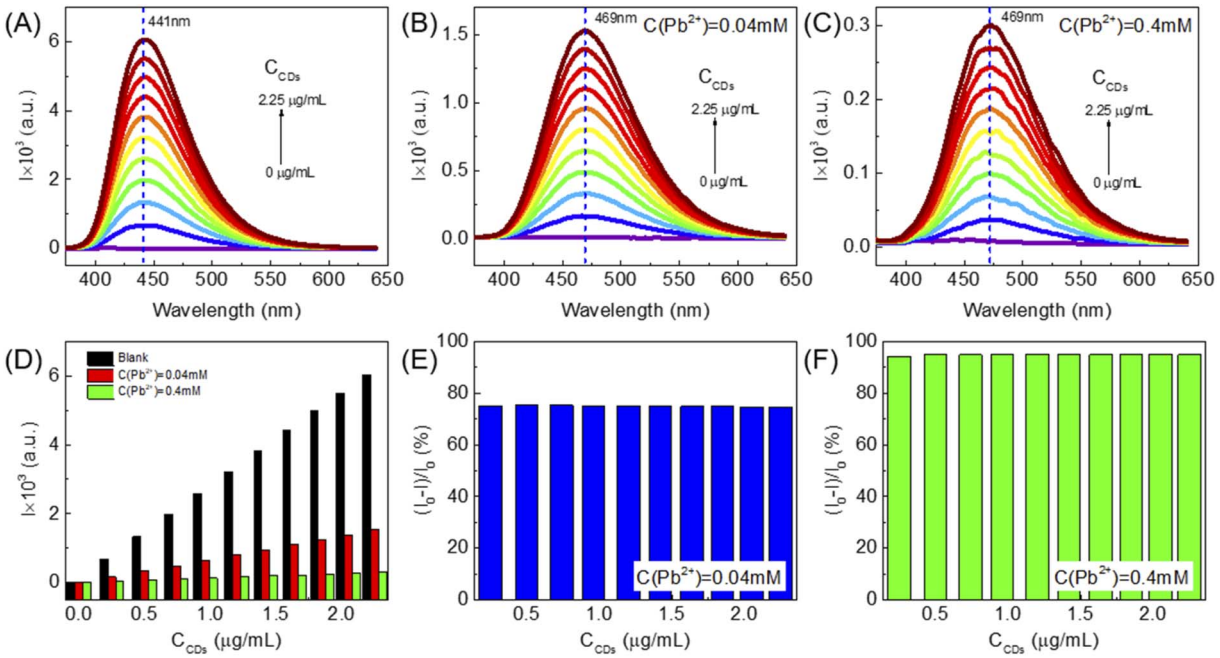

Fig. 3 Influence of U-CDs concentration on fluorescence quenching degree. (A) The fluorescence spectra of blank U-CDs of different concentrations. (B) The fluorescence spectra of the U-CDs reacting with 0.04 mM Pb^{2+} and (C) 0.4 mM Pb^{2+}. (D) Their PL intensities as functions of U-CDs concentration. The fluorescence quenching degrees $(I_0 - I)/I_0$ for 0.04 mM Pb^{2+} (E) and 0.4 mM Pb^{2+} (F).

independent of the concentration of U-CDs. In addition, it is found that the emission peaks are red-shifted from 441 nm to 469 nm under both Pb^{2+} concentrations.

3.4 Pb^{2+} detection

Some trace metal ions can cause fluorescence quenching of QDs, which can be used for the detection of these metal ions. Similarly, fluorescent U-CDs can be used for the detection of heavy metal ions. Here, we first prepared with standard curve using the U-CDs solution of 1.12 μg mL^{-1} ($I_0 = 3000$ a.u.), which reacted with Pb^{2+} solution with different concentrations. The fluorescence spectra were recorded as shown in Fig. 4A. For comparison, another two group of experiments were conducted using U-CDs solutions with different concentrations, 0.37 μg mL^{-1} ($I_0 = 1000$ a.u.) and 2.23 μg mL^{-1} ($I_0 = 6000$ a.u.) respectively. The obtained PL spectra were shown in Fig. 4B and C respectively. For the first group of experiment, the relationship between the PLQD of U-CDs and $[Pb^{2+}]$ can be well described by the Stern–Volmer equation as $(I_0/I - 1) = 53.001\,[Pb^{2+}]$ when $[Pb^{2+}]$ is 0.04–0.36 mM, and the correlation coefficient was $R^2 = 0.9996$. The limit of detection (LOD) is calculated to be 1 μM, furthermore, for the other two groups of experiments, their standard curves basically coincide with that of the first group (Fig. 4D), indicating that the concentration of U-CDs has little effect on the standard curve, which is extremely useful for practical application. It allows a long interval between standard curve preparation and actual detection. Furthermore, both are allowed to performed under different U-CDs concentrations, which causes less influence on the accuracy of the detection results.

3.5 Possible PL quenching mechanism of U-CDs

The fluorescence quenching degree of U-CDs is independent of the concentration of U-CDs, which may be related to the particularity of U-CDs used in this experiment. In this work, the U-CDs were synthesized under optimal reaction condition with high PLQY (~100%). Therefore, the U-CDs solution with very low concentration also keeps a considerable PL intensity. As mentioned above, the absorbance peak at 360 nm is basically coincident with the excitation peak, which is the characteristic absorption peak of the U-CDs, which is contributed from the n → π* electronic transition of the surface functional group –C=O of the U-CDs, suggesting that the amide bond might be a part of fluorophore. The lone pair of electrons on the nitrogen (N) atom of the amide bond are easy to complex with Pb^{2+} ion, which destroys the charge transfer on the amide bond and leads to the PL quenching of the U-CDs, as shown in Fig. 5.

The binding of metal ions to the U-CDs results in the PL quenching can be expressed in eqn (2).

$$\text{U-CD} + Pb^{2+} \rightleftarrows {}^{K}\text{U-CD}\cdots Pb^{2+} \quad (2)$$

When the reaction reaches equilibrium, the reaction equilibrium constant K can be expressed as follows,

$$K = \frac{[\text{U-CD}\cdots Pb^{2+}]}{[\text{U-CD}][Pb^{2+}]} \quad (3)$$

Suppose the metal ions are far more than the U-CDs. With a small increase or decrease in the number of U-CDs, the concentration of metal ions around each CD is almost

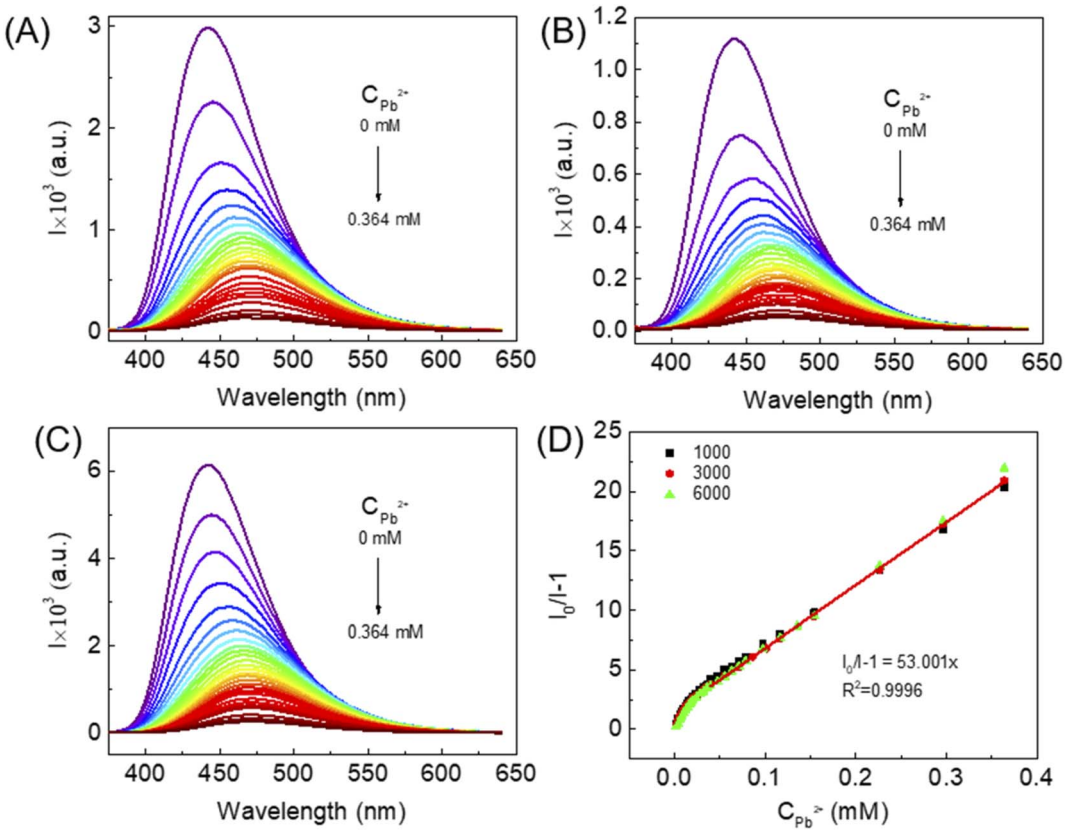

Fig. 4 PL spectra of U-CDs with initial PL intensities of (A) $I_0 = 3000$ a.u. (B) $I_0 = 1000$ a.u. (C) $I_0 = 6000$ a.u. reacting with Pb^{2+} with different concentrations. (D) Standard curves fitted by Stern–Volmer equation.

unchanged. Therefore, the number of metal ions bound to each U-CD particle is only related to the concentration of metal ions. The larger concentration of metal ions allows more the number of metal ions bound on the surface of U-CDs, resulting in greater fluorescence quenching degree. Therefore, the fluorescence quenching degree of U-CDs is independent of the concentration of U-CDs, which is determined by the concentration of metal ions. However, this is just speculation, and more experimental or theoretical evidences are needed.

3.6 Selectivity of metal ions

Herein, a selectivity experiment was performed under U-CDs concentration of 2.23 μg mL^{-1} (I_0 = ~6000 a.u.). Some

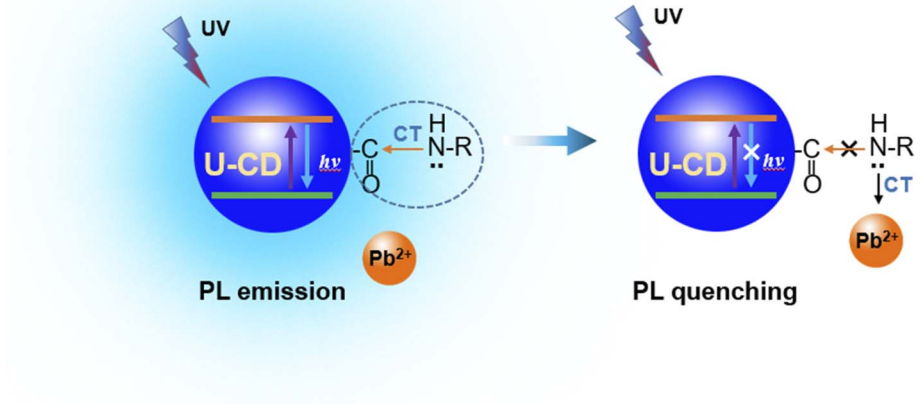

Fig. 5 Schematic diagram of possible PL quenching mechanism of U-CDs.

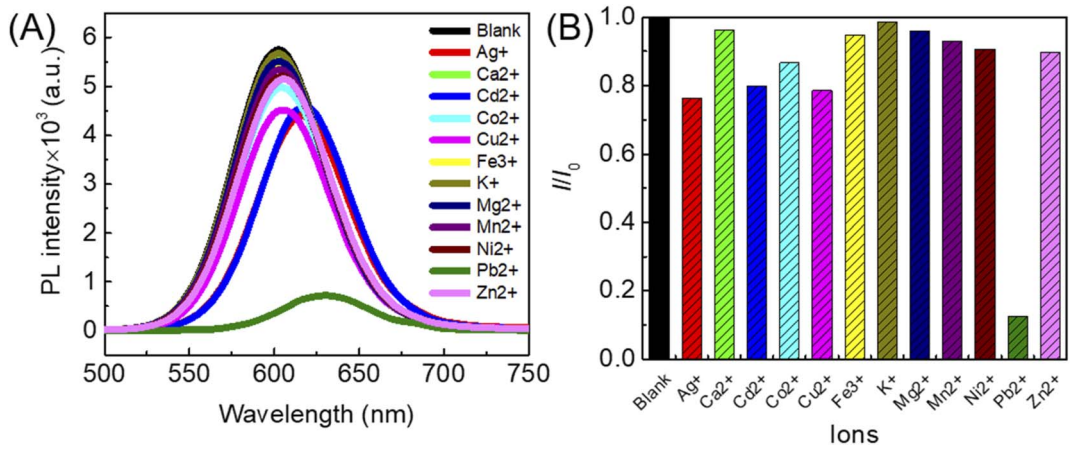

Fig. 6 Selective detection of CDs on metal ions. (A) Fluorescence spectra of CDs after reaction with different metal ions. (B) Corresponding relative fluorescence intensity I/I_0 at relative higher concentration of CDs.

Table 1 Pb^{2+} recovery analysis

Number	Concentration of U-CDs/(μg mL^{-1})	Adding quantity/(μM)	Recovery quantity/(μM)	Recovery rate/%	RSD/%
1	0.74	50.00	42.55	85.1	1.3
2	0.74	100.00	83.25	83.3	2.2
3	0.74	300.00	251.04	83.7	1.8
4	1.41	50.00	45.28	90.6	1.4
5	1.41	100.00	85.58	85.6	2.2
6	1.41	300.00	260.02	86.7	7.2

common metal ions were chosen for the selectivity experiment. The acquired fluorescence spectra are displayed in Fig. 6A, and the relative fluorescence intensities are shown in Fig. 6B. It is clear that Pb^{2+} induces the most significant PL quenching degree on U-CDs, suggesting that the U-CDs have a certain selectivity for Pb^{2+}.

3.7 Recovery analysis

In order to verify the practicability and accuracy of the U-CDs as fluorescence sensors, the established detection method was applied to the recovery analysis of Pb^{2+} in water samples. Two U-CDs solutions with concentrations as 0.74 μg mL^{-1} and 1.41 μg mL^{-1} respectively were used to detect the Pb^{2+} solutions with low, middle, and high concentrations respectively. Each metal ion concentration was measured three times in parallel, and the recovery rate and relative standard deviation were calculated. The results are shown in Table 1, and the recovery rate ranges from 83.3% to 90.6%, suggesting that the proposed analysis method can well detect Pb^{2+} in water samples, and the detection error is less than 20%.

4 Conclusions

In this work, when studying the interactions between metal ions and U-CDs, we found that the degree of fluorescence quenching is independent of the concentration of U-CDs. This feature provides great convenience for practical applications. It is not necessary to optimize the concentration of U-CDs and allows a long interval between standard curve preparation and actual detection. Even if the U-CDs concentrations for the standard curve preparation and actual detection are different, relatively accurate results can be obtained with acceptable error, which greatly improves the detection efficiency. Based on the experimental observations, we proposed a possible mechanism to explain this phenomenon. To our best knowledge, this work has never been reported before and provides a new idea for the design of novel fluorescent sensors.

Author contributions

Shaogui Wu and Jiayang Wang: conceptualization. Xiang Long, Ruixue Li and Jiamei Xiang: experiment, writing – original draft. Shaogui Wu: review & editing.

Conflicts of interest

There are no conflicts to declare.

Acknowledgements

This work was supported by Project of Science and Technology Department of Sichuan Province, China (No. 2021JDR0131, 21RKX0358).

References

1 Y. Chen and Z. Rosenzweig, *Anal. Chem.*, 2002, **74**, 5132–5138.
2 X. Wang, A. Dong, Y. Hu, J. Qian and S. Huang, *Chem. Commun.*, 2020, **56**, 10809–10823.
3 G. Wang, M. Yu and X. Feng, *Chem. Soc. Rev.*, 2021, **50**, 2388–2443.
4 Y.-P. Sun, B. Zhou, Y. Lin, W. Wang, K. S. Fernando, P. Pathak, M. J. Meziani, B. A. Harruff, X. Wang and H. Wang, *J. Am. Chem. Soc.*, 2006, **128**, 7756–7757.
5 Z. Kang and S.-T. Lee, *Nanoscale*, 2019, **11**, 19214–19224.
6 H. Liu, T. Ye and C. Mao, *Angew. Chem.*, 2007, **119**, 6593–6595.
7 S. N. Baker and G. A. Baker, *Angew. Chem., Int. Ed.*, 2010, **49**, 6726–6744.
8 Z. Yang, Z. Li, M. Xu, Y. Ma, J. Zhang, Y. Su, F. Gao, H. Wei and L. Zhang, *Nano-Micro Lett.*, 2013, **5**, 247–259.
9 D. Xiao, D. Yuan, H. He and J. Lu, *Luminescence*, 2013, **28**, 612–615.
10 K. Jiang, S. Sun, L. Zhang, Y. Lu, A. Wu, C. Cai and H. Lin, *Angew. Chem.*, 2015, **127**, 5450–5453.
11 Z. Li, L. Wang, Y. Li, Y. Feng and W. Feng, *Mater. Chem. Front.*, 2019, **3**, 2571–2601.
12 H. Wang, C. Sun, X. Chen, Y. Zhang, V. L. Colvin, Q. Rice, J. Seo, S. Feng, S. Wang and W. Y. William, *Nanoscale*, 2017, **9**, 1909–1915.
13 D. Sun, R. Ban, P.-H. Zhang, G.-H. Wu, J.-R. Zhang and J.-J. Zhu, *Carbon*, 2013, **64**, 424–434.
14 H. Wang, P. Sun, S. Cong, J. Wu, L. Gao, Y. Wang, X. Dai, Q. Yi and G. Zou, *Nanoscale Res. Lett.*, 2016, **11**, 1–6.
15 H. Luo, Q. Guo, P. Á. Szilágyi, A. B. Jorge and M.-M. Titirici, *Trends Chem.*, 2020, **2**, 623–637.
16 K. W. Kim, T.-Y. Choi, Y. M. Kwon and J. Y. H. Kim, *Electron. J. Biotechnol.*, 2020, **47**, 36–42.
17 S. S. Arumugam, J. Xuing, A. Viswadevarayalu, Y. Rong, D. Sabarinathan, S. Ali, A. A. Agyekum, H. Li and Q. Chen, *J. Photochem. Photobiol., A*, 2020, **401**, 112788.
18 R. Guo, X. Liu, B. Wen, F. Liu, J. Meng, P. Wu, J. Wu, Q. Li and L. Mai, *Nano-Micro Lett.*, 2020, **12**, 1–12.
19 N. Puvvada, B. P. Kumar, S. Konar, H. Kalita, M. Mandal and A. Pathak, *Sci. Technol. Adv. Mater.*, 2012, **13**(4), 045008.
20 B.-B. Wang, J.-C. Jin, Z.-Q. Xu, Z.-W. Jiang, X. Li, F.-L. Jiang and Y. Liu, *J. Colloid Interface Sci.*, 2019, **551**, 101–110.
21 B. Wang, Y. Chen, Y. Wu, B. Weng, Y. Liu, Z. Lu, C. M. Li and C. Yu, *Biosens. Bioelectron.*, 2016, **78**, 23–30.
22 Q. Xu, P. Pu, J. Zhao, C. Dong, C. Gao, Y. Chen, J. Chen, Y. Liu and H. Zhou, *J. Mater. Chem. A*, 2015, **3**, 542–546.
23 L. T. Da, F. Pardo-Avila, L. Xu, D. A. Silva, L. Zhang, X. Gao, D. Wang and X. H. Huang, *Nat. Commun.*, 2016, **7**, 11244.
24 D. Qu, M. Zheng, L. Zhang, H. Zhao, Z. Xie, X. Jing, R. E. Haddad, H. Fan and Z. Sun, *Sci. Rep.*, 2014, **4**, 1–11.
25 S. Wu, C. Zhou, C. Ma, Y. Yin and C. Sun, *J. Chem.*, 2022, **2022**, 3737646.
26 H. N. Kim, W. X. Ren, J. S. Kim and J. Yoon, *Chem. Soc. Rev.*, 2012, **41**, 3210–3244.
27 L. Chai, Z. Hu, X. Wang, L. Zhang, T.-T. Li, Y. Hu, J. Pan, J. Qian and S. Huang, *Carbon*, 2021, **174**, 531–539.
28 Y. Zhang, X. Liu, Y. Fan, X. Guo, L. Zhou, Y. Lv and J. Lin, *Nanoscale*, 2016, **8**, 15281–15287.